Cardiovascular Engineering and Technology, Vol. 10, No. 3, September 2019 *(© 2019)* pp. 500–507
https://doi.org/10.1007/s13239-019-00417-2

Fabrication of Low-Cost Patient-Specific Vascular Models for Particle Image Velocimetry

KATRINA L. RUEDINGER [1,3], RAFAEL MEDERO [2,3] and ALEJANDRO ROLDÁN-ALZATE [1,2,3]

[1]Department of Biomedical Engineering, University of Wisconsin-Madison, Madison, WI, USA; [2]Department of Mechanical Engineering, University of Wisconsin-Madison, Madison, WI, USA; and [3]Department of Radiology, WIMR, University of Wisconsin-Madison, 2476, 1111 Highland Ave, Madison, WI 53705, USA

(Received 6 March 2019; accepted 6 May 2019; published online 16 May 2019)

Associate Editor Ajit P. Yoganathan oversaw the review of this article.

Abstract

Purpose—Particle image velocimetry (PIV), an *in vitro* experimentation technique that optically measures velocity components to analyze fluid velocity fields, has become increasingly popular to study flow dynamics in various vascular territories. However, it can be difficult and expensive to create patient-specific clear models for PIV due to the importance of refractive index matching of the model and the fluid. We aim to implement and test the use of poly-vinyl alcohol (PVA) in a lost-core casting technique to create low-cost, patient-specific models for PIV.

Methods—Anonymized patient vascular anatomies were segmented and processed in Mimics/3Matic to create patient-specific cores from 3D digital subtraction angiographies. The cores were 3D-printed with PVA and post-processed with a 80:20 water:glue mixture to smooth the surface. Two silicones, Sylgard 184 and Solaris, were used to encapsulate the model and the PVA core was dissolved using warm water. Computed tomography scans were used to evaluate geometric accuracy using circumferences and surface differences in the model.

Results—Mean geometric differences in circumference along the inlet centerline and the mean surface difference in the aneurysm between the final Silicone Model and the desired STL Print geometry were statistically insignificant (0.6 mm, 95% CI [− 1.4, 2.8] and 0.3 mm 95% CI [− 0.1, 0.7], respectively). Particle illumination within each model was successful. The cost of one 10 cm × 10 cm × 5 cm model was $69.

Conclusion—This technique was successful to implement and test the use of PVA in a lost-core casting technique to create low-cost, patient-specific *in vitro* models for PIV experimentation.

Keywords—Particle image velocimetry, Patient-specific, Compliant vascular model, 3D printing.

Address correspondence to Alejandro Roldán-Alzate, Department of Radiology, WIMR, University of Wisconsin-Madison, 2476, 1111 Highland Ave, Madison, WI 53705, USA. Electronic mail: roldan@wisc.edu

INTRODUCTION

Particle image velocimetry (PIV) is an *in vitro* experimental technique that optically measures fluid velocity fields by tracking particle displacements with high spatial and temporal resolution.[19] This technique requires clear models so high-speed cameras can track particles that are illuminated by a laser. In addition, models need to match the refractive index (RI) of the working fluid to avoid image distortion between the solid–liquid interface in order to accurately measure entire velocity fields.[31]

In biomechanics, PIV is helpful to capture complex physiological flow patterns in various vascular territories and has been compared to flows gathered from medical imaging techniques, such as magnetic resonance image (MRI).[10,13,15,17,29] This requires anatomically realistic *in vitro* models, however, these can be difficult to manufacture and are prohibitively expensive as offered by commercial vendors.

Yazdi *et al.* presented a review on the use of rigid and compliant *in vitro* phantoms for hemodynamic analysis in the vascular system with PIV and emphasized the breadth of prototyping, manufacturing, and RI matching techniques currently used.[33] PIV analysis has previously been done with 3D-printed patient-specific rigid models; however, these materials tend to have a high RI relative to water (1.33), which makes fluid-material index matching difficult without the use of hazardous chemicals such as sodium iodide.[2,22] Another limitation of rigid materials is the lack of distensibility, which poorly represents the *in vivo* conditions.[8]

On the other hand, compliant *in vitro* patient-specific models provide more realistic mechanical properties and are most commonly made with Sylgard 184 (Dow Corning, Midland, MI) due to its low RI.[33] A lost-core casting technique has been used to create compliant models, with cores made from wax, low melting point alloys or even chocolate.[7,16,18,23,25,26,28,32] One disadvantage of these materials is the need for a mold to form the core, which adds complexity and manufacturing time, especially when creating patient-specific silicone models. A variety of new 3D-printed materials have been introduced to print the cores without the need for a mold, however, they still require chemical solutions that alter the properties of water to dissolve the core from the silicone.[1,4,11,34]

In this short communication, we introduce polyvinyl alcohol (PVA), a water-soluble material used to print support structures in fused deposition modeling (FDM), to directly print cores without the need for a mold or other chemical solutions to dissolve. Although never used as the 3D-printed core, PVA was previously used as a wall in a rigid phantom and to polish cores before casting in compliant phantoms.[3,5,8,14] By capitalizing on the purely water-soluble 3D-printed material and the applicability of this method for many castable materials, we aim to implement and test the use of PVA as a 3D-printed core to create low-cost, patient-specific, *in vitro* vascular models for analysis with PIV.

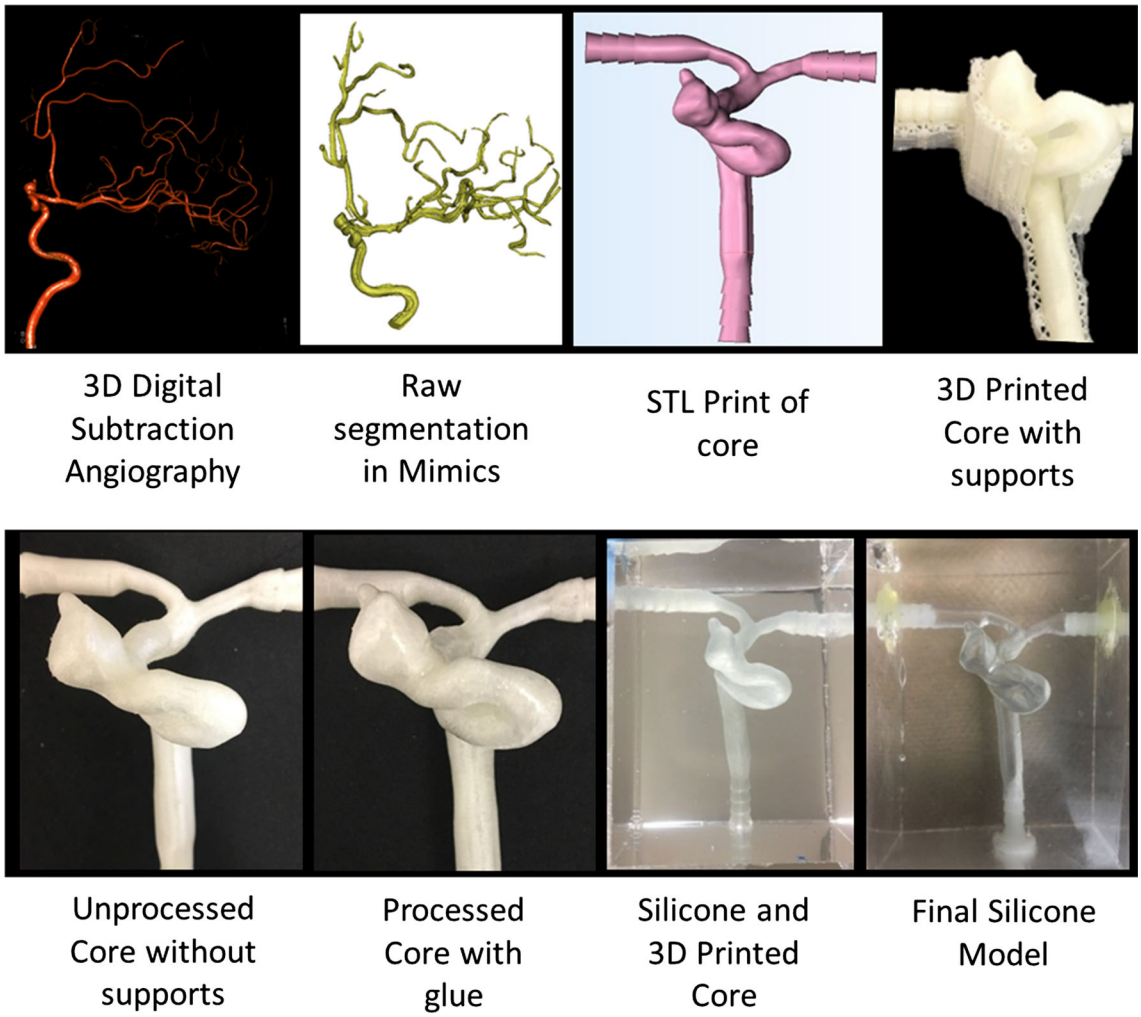

FIGURE 1. Model making process is illustrated with a patient-specific intracranial aneurysm. Projections from an anonymized 3D DSA acquisition were selected from an in-house database with IRB approval. Segmentation of the vascular anatomy was done with Mimics, model scaling (× 2) and connectors were added with 3-Matic to create the STL Print of the core. The patient-specific vascular core was then 3D printed out of PVA using the Ultimaker 3+ Extended. The supports were carefully removed to create the Unprocessed Core. The 3D Printed Core was coated in a thin layer of glue to create the Processed Core. The processed core was submerged in silicone. The final Silicone Model with the PVA core was dissolved out with water.

TABLE 1. 3D printer parameters for the Ultimaker 3+ Extended used to create the patient-specific cores out of PVA.

Settings used to print PVA cores on the Ultimaker 3+ extended			
Diameter filament	2.85 mm	Printing temperature	215 °C
Nozzle size	0.4 mm	Build plate temperature	60 °C
Layer height	0.1 mm	Fan cooling speed	50%
Infill density	10%	Support pattern	Triangles
Printing speed	35 mm/s	Support placement	Touching buildplate

METHODS

There are four main steps to fabricate these models: anatomy segmentation, 3D-printing of the patient-specific core, silicone casting, and core removal. Gloves are worn during casting and the removal of the core for safety as well as to decrease finger prints on the silicone models which may disrupt PIV results.

Anatomy Segmentation

Anonymized digital-subtraction angiography acquisitions of three intracranial aneurysms were retrospectively obtained from an in-house database after IRB approval. Each image dataset was imported into Mimics (Materialise, Leuven, Belgium) and segmented using global thresholding, region growing and manual selection, if needed, to create a 3D volume (Fig. 1). Each volume was imported into 3-Matic (Materialise, Leuven, Belgium) for smoothing of the coarse walls (Laplacian (1st and 2nd Order) smoothing operations) and the addition of barbed connectors to create the patient-specific virtual model of the core (Fig. 1). Here the model was left true-to-size or scaled by 2. The surface of the patient-specific cores was exported in stereolithography (STL) format.

3D-PRINTED PATIENT-SPECIFIC CORE

All cores were printed out of PVA using an FDM printer (Ultimaker 3+ Extended, Cambridge, MA) with the parameters described in Table 1 and an oblique orientation with respect to the build plate. Once finished, the supports were manually separated from the core to create the Unprocessed Core (Fig. 1). To improve the surface quality, a thin layer of diluted polyvinyl acetate glue (80:20, glue:water) (Elmer's Products, High Point, NC) was applied to the core to create the Processed Core with glue.

Silicone Casting

A five-sided acrylic box was created based on the specific dimensions of each core geometry. Acrylic pieces were placed and adhered together using hot melt adhesive to create a watertight box. The box was cleaned and the PVA core was secured to the walls at the appropriate height using the hot melt adhesive. Models were made out of two silicone materials: Sylgard 184 and Solaris (Smooth-On, Macungie, PA). Properties of both silicones can be found in Table 2.[12,24,27,30] Both were prepared according to instructions (Sylgard 184: 10A:1B ratio and Solaris: 1A:1B ratio) and were placed in a vacuum to remove bubbles before pouring over the Processed Core in the acrylic box. The silicone was left to cure for 48 h at room temperature.

TABLE 2. Mechanical and physical properties of the Sylgard 184 and Solaris silicones.[9,13,15,17]

	Sylgard 184	Solaris
Index of refraction	1.412	1.410
Modulus (MPa)	1.32–1.84	0.14–0.17
Ultimate tensile strength (MPa)	5.13–7.07	1.24
Shore hardness	43	15

Core Removal

Once the silicone cured, the acrylic box was carefully disassembled by removing the hot melt adhesive leaving a silicone block (Fig. 1). Using small tools, the PVA material was removed from the outlets by twisting and breaking off the material. Then warm water was then inserted and continuously run through the core to saturate the PVA. Once saturated, the PVA dissolved leaving a smooth lumen inside of the silicone (Fig. 1).

PIV Compatibility

Two true-size silicone models made with Sylgard 184 and Solaris were tested for PIV compatibility. The RI of a fluid mixture containing glycerol and water was measured using a digital refractometer (Fisherbrand, Fischer Scientific, Pittsburgh, PA) to ensure index matching with the models. Image distortion was tested by filling both models with this fluid mixture after

polyamide particles (diameter = 20 mm) were added. The particles were illuminated with a 527 nm ND:YLF laser (Photonics Industries International, Inc., Long Island, NY) and images were acquired with a high-speed camera (Phantom v341, Vision Research, Wayne, NJ).

Geometric Comparison

The Unprocessed PVA Core (without glue), Processed PVA Core (with glue), and the final Silicone Model (a Sylgard 184 model of a scaled ×2 aneurysm) were imaged with a CT scanner (Discovery CT750 HD, GE Healthcare, Chicago, IL) (0.15 × 0.15 × 0.315 mm resolution) to analyze the geometric accuracy of each step. The DICOM images obtained from the scan of each model was imported into Mimics for segmentation and analysis. Due to the clear attenuation difference between air and PVA or silicone, threshold segmentation was done and confirmed by measuring an external connector. A centerline was generated from Mimics for each model and the circumferences along the inlet centerline were exported at 2 mm increments. Additionally, the surface of the aneurysm from the final Silicone Model was compared to surface of the aneurysm from the STL Print of the core to observe any geometric differences.

Statistical Analysis

Qualitative and quantitative differences in the circumference along the centerline of the inlet of the model were used to compare each step in the model making process (Unprocessed core, Processed Core, final Silicone Model) with the STL Print of the core. The average difference between the Unprocessed Core, Processed Core, and final Silicone Model were reported and statistical significance was defined with a confidence interval of 95%. Qualitative and quantitative comparisons of aneurysm surface differences between the final Silicone Model and the STL Print were also done.

RESULTS

The fabrication of patient-specific models using a lost-core casting technique with a 3D-printed PVA Core was successful for intracranial aneurysms (both true-size and × 2). The same technique was used with both casting materials, Sylgard 184 and Solaris, and the difference in silicone mechanical properties, as stated in Table 2, was palpable.

Centerlines were created through the inlet of the Unprocessed PVA Core, Processed PVA Core, and the final Silicone Model obtained from CT. The circumference along the inlet centerline was chosen for analysis since the patient-specific inlet cross section is not a complete circle. Figure 2 illustrates the circumferences (mm) along the inlet centerline of each model making step. The STL Print of the core (red triangles) represents the ideal geometry and the Silicone Model represents the final compliant, *in vitro* model for PIV (green triangles). The mean difference in circumference along the inlet centerline between the Final Silicone Model and STL print was 0.6 mm, 95% CI [− 1.4, 2.8]. The mean difference between the Unprocessed Core (without glue) and the STL Print was 2.1 mm, 95% CI [− 2.4, 6.6] and the Processed Core (with glue) and the STL Print was 3.5 mm, 95% CI [0.9, 6.2].

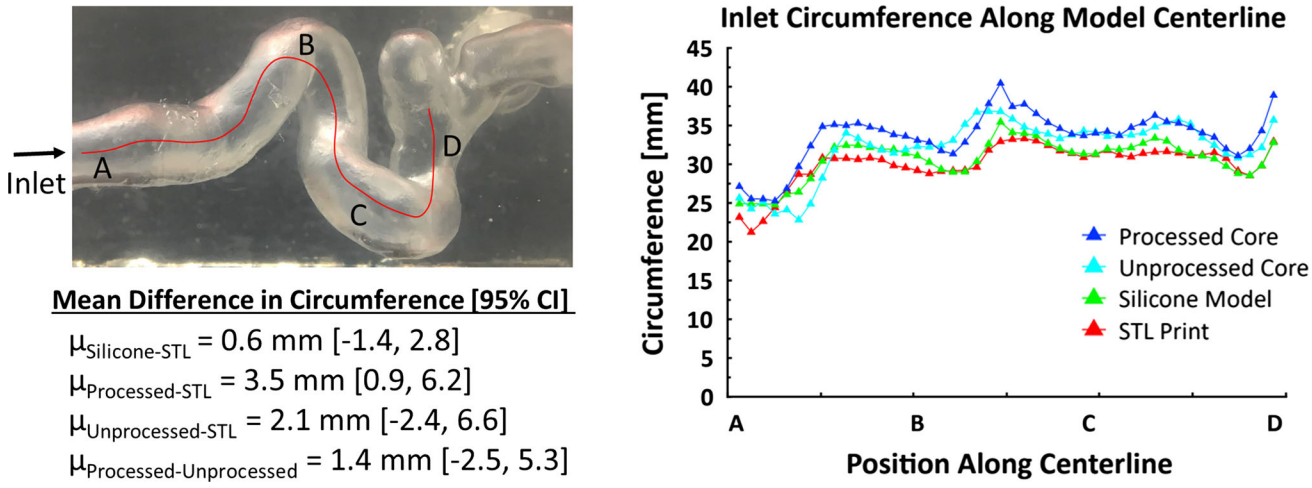

FIGURE 2. Comparison of the geometric circumference along the centerline along the inlet of the × 2 model from points A–D at four different model making steps: unprocessed core, processed core, final silicone model and the STL Print of the core. Circumferences were derived from CT images of the physical parts (resolution 0.15 × 0.15 × 0.315 mm). Centerlines were created in mimics.

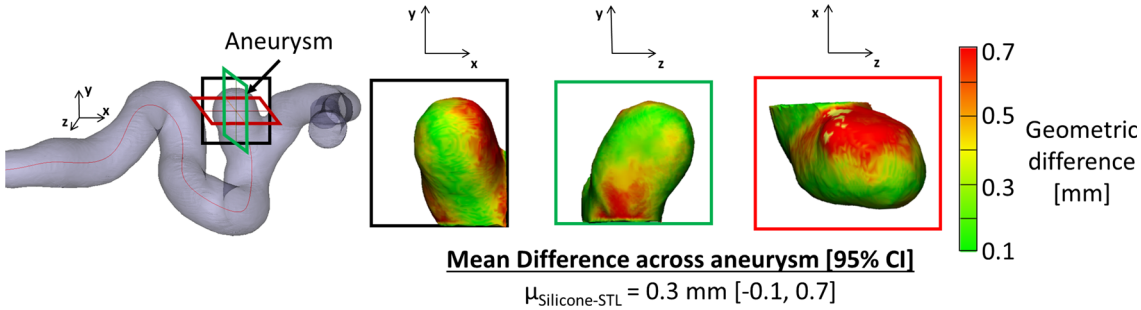

FIGURE 3. Comparison of geometric differences in diameter in the aneurysm between the final silicone model and the ideal STL print. Spatial differences (mm) are illustrated with the color bar where red is the area with greatest difference. Geometry subtractions were done in 3-Matic.

Finally, the mean difference in circumference along the inlet between the Unprocessed Core (without glue) and the Processed Core (with glue) was 1.4 mm, 95% CI [− 2.5, 5.3].

Absolute geometric differences in the surface of the aneurysm between the final Silicone Model and the STL Print ranged from 0 to 0.7 mm with a mean difference of 0.3 mm, 95% CI [− 0.1, 0.7] (Fig. 3). All mean differences in circumference along the inlet centerline and the aneurysm surface comparison were deemed insignificant, except for the difference between the Processed Core and the STL Print.

Particle illumination was tested in the real-size aneurysm model made with both Sylgard 184 and Solaris. Both models were successfully index matched with a 58:42 glycerol:water mixture (RI = 1.412 nm) and the particles were imaged without distortion or light scattering at the wall of the inlet (red box) of both models (Fig. 4).

The overall time required to make the models varied based on the size of the anatomy and availability of resources. For instance, the scaled intracranial aneurysm PVA core in Fig. 1 required ~ 5 h to print and required 4 days to complete (segmentation, printing and casting were completed in 2 days and 2 days of silicone curing). It was also found that PVA rolls which were connected to the printer for a long period of time had more failed prints than PVA rolls which were stored in a dry area. This was likely due to the saturation of the PVA rolls.

The cost of the 3D-printed PVA core was less than $5 for each anatomy. As the size of the anatomy varied, so did the size of the entire model and therefore, the amount of silicone needed was the largest factor in the total cost of the model. For the 8 cm × 8 cm × 7 cm (Fig. 1) and the 10 cm × 10 cm × 5 cm model (Fig. 2) the total cost of the models were estimated to be around $62–$69 (Sylgard 184 = ~ $0.128/mL). The Solaris silicone cost $0.05/mL, making those models even cheaper ($25–$28).

DISCUSSION

This article presents the use of 3D-printed patient-specific anatomy cores made from PVA to create low-cost patient-specific *in vitro* models for PIV experimentation. The use of PVA in a lost-core casting technique has been successfully implemented and tested for geometric accuracy and PIV compatibility. Sylgard 184 was chosen to compare for geometric accuracy because of its most extensive use for models in the PIV community.[33] The greatest geometric difference, 3.5 mm, occurred between the Processed Core and the STL Print, concluding that the addition of 80:20, water:glue, made a significant difference to the STL Print of the core. Since this is a circumference measurement, the estimated mean difference in diameter was ~ 0.1 mm. This is larger than the previously reported 0.01 mm difference in a straight tube.[9] This geometry change, however, was minimized once the processed core was submerged into the silicone, suggesting that the PVA core and water soluble glue absorbed some of the silicone to bring the final Silicone Model geometry back down to the desired STL Print size.

Although the model making process presented here focuses on intracranial aneurysms, this technique was also successful in two other anatomical territories derived from MRI (a brain ventricle and a portal vein) (Fig. 5). The portal vein silicone model was successfully used for PIV analysis to compare flow patterns at different resolutions with MRI and computational fluid dynamic simulations.[21]

Compared to other compliant *in vitro* phantoms creation techniques, this method provides a novel way of printing the core anatomy with PVA and dissolving it out of a silicone block with only water. Additionally, the ability to use this technique with a more compliant silicone, such as Solaris, may allow users more material variability for PIV experimentation.

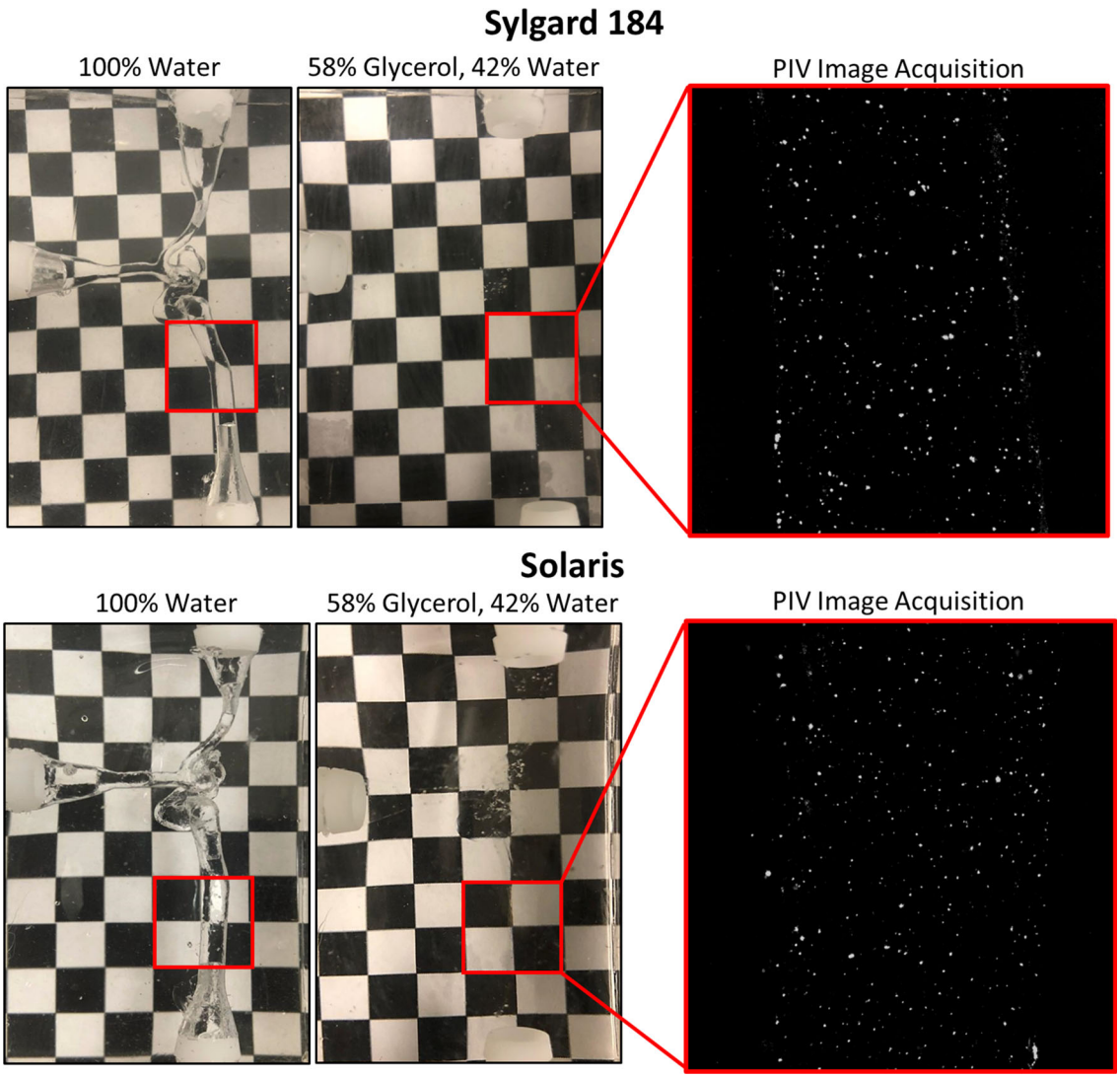

FIGURE 4. Distortion of checkerboard shown through the compliant intracranial aneurysm silicone models made of Sylgard 184 and Solaris and filled with either water or a 58:42 glycerol:water mixture. Red box highlights the area of the inlet where the particles were illuminated to reveal no particle distortion and no light scattering at the solid–liquid interface.

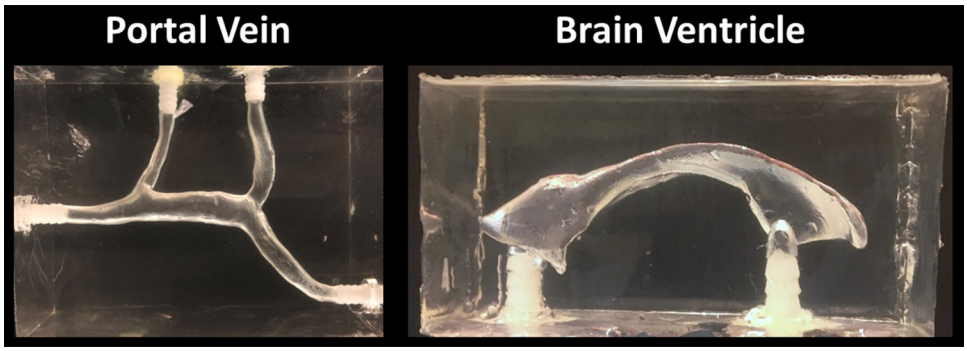

FIGURE 5. Final *in vitro* compliant silicone models (Sylgard 184) of a patient-specific portal vein and brain ventricle made with a 3D-printed PVA core.

The presented method to create the PVA cores is limited by the size of the 3D-printer's build volume, 197 × 215 × 300 mm. Therefore, anatomies larger than this build volume may need to be isolated into sections if the Ultimaker 3+ is used. Also, it is important to note that different segmentation or post-processing techniques may produce a varied patient-specific anatomy.[6,20] The method outlined here uses a 3D-DSA where contrast has enhanced the vasculature of interest which aids in vessel segmentation; however, geometric differences due to segmentation may remain. The Solaris silicone required more careful core extraction since the material was soft and more easily da-mageable by sharp extraction tools. Within the core and casting process, additional manufacturing artifacts such as debris or fingerprints were present but can be avoided by wearing gloves, improving the application of the polyvinyl acetate glue, and covering the silicone mold while curing.

CONCLUSION

Overall, this technique demonstrates a lost-core casting method of creating compliant, patient-specific *in vitro* vascular models for analysis with PIV. The novelty of this technique involves the use of PVA to 3D-print the core anatomy, which is both a low-cost material and is easily extracted from the model using warm water. Also, the ability to apply this process with the Solaris silicone in addition to Sylgard 184, provides the opportunity for use of other silicone elastomers for *in vitro* PIV experimentation.

ACKNOWLEDGEMENTS

Funding for this project was partially supported by a National Institutes of Health K12-DK100022 Grant (Dr. Roldán-Alzate).

AUTHOR CONTRIBUTIONS

All authors have contributed to the material presented in this manuscript and this material has not been submitted for publication elsewhere.

CONFLICT OF INTEREST

K.L. Ruedinger, R. Medero and A. Roldán-Alzate declare that they have no conflicts of interest to report.

REFERENCES

[1]Arcaute, K., and R. B. Wicker. Patient-specific compliant vessel manufacturing using dip-spin coating of rapid prototyped molds. *J. Manuf. Sci. Eng.* 130:1–13, 2008.
[2]Bai, K., and J. Katz. On the refractive index of sodium iodide solutions for index matching in PIV. *Exp. Fluids* 55:1–6, 2014.
[3]Brunette, J., R. Mongrain, and J. C. Tardif. A realistic coronary artery phantom for particle image velocimetry. *J. Vis.* 7:241–248, 2004.
[4]Buchoux, A., P. Valluri, S. Smith, A. A. Stokes, P. R. Hoskins, and V. Sboros. Manufacturing of microcirculation phantoms using rapid prototyping technologies. In: Proceedings of Annual International Conference of the IEEE Engineering in Medicine and Biology Society, pp. 5908–5911, 2015.
[5]Büsen, M., T. A. S. Kaufmann, M. Neidlin, U. Steinseifer, and S. J. Sonntag. In vitro flow investigations in the aortic arch during cardiopulmonary bypass with stereo-PIV. *J. Biomech.* 48:2005–2011, 2015.
[6]Despotović, I., B. Goossens, and W. Philips. MRI segmentation of the human brain: Challenges, methods, and applications. *Comput. Math. Methods Med.* 2015:1–23, 2015.
[7]Ford, M. D., H. N. Nikolov, J. S. Milner, S. P. Lownie, E. M. DeMont, W. Kalata, F. Loth, D. W. Holdsworth, and D. A. Steinman. PIV-measured versus CFD-predicted flow dynamics in anatomically realistic cerebral aneurysm models. *J. Biomech. Eng.* 130:021015, 2008.
[8]Geoghegan, P. H., N. A. Buchmann, J. Soria, and M. C. Jermy. Time-resolved PIV measurements of the flow field in a stenosed, compliant arterial model. *Exp. Fluids* 54:1–19, 2013.
[9]Geoghegan, P. H., N. A. Buchmann, C. J. T. Spence, S. Moore, and M. Jermy. Fabrication of rigid and flexible refractive-index-matched flow phantoms for flow visualisation and optical flow measurements. *Exp. Fluids* 52:1331–1347, 2012.
[10]Gülan, U., B. Lüthi, M. Holzner, A. Liberzon, A. Tsinober, and W. Kinzelbach. Experimental study of aortic flow in the ascending aorta via Particle Tracking Velocimetry. *Exp. Fluids* 53:1469–1485, 2012.
[11]Hütter, L., P. H. Geoghegan, P. D. Docherty, M. S. Lazarjan, and D. Clucas. Fabrication of a compliant phantom of the human aortic arch for use in Particle Image Velocimetry (PIV) experimentation. *Curr. Dir. Biomed. Eng.* 2:493–497, 2016.
[12]Johnston, I. D., D. K. McCluskey, C. K. L. Tan, and M. C. Tracey. Mechanical characterization of bulk Sylgard 184 for microfluidics and microengineering. *J. Micromech. Microeng.* 24:1–7, 2014.
[13]Kitajima, H. D., K. S. Sundareswaran, T. Z. Teisseyre, G. W. Astary, W. J. Parks, O. Skrinjar, J. N. Oshinski, and A. P. Yoganathan. Comparison of Particle Image Velocimetry and Phase Contrast MRI in a Patient-Specific Extracardiac Total Cavopulmonary Connection. *J. Biomech. Eng.* 130:041004, 2008.
[14]Laumen, M., T. Kaufmann, D. Timms, P. Schlanstein, S. Jansen, S. Gregory, K. C. Wong, T. Schmitz-Rode, and U. Steinseifer. Flow analysis of ventricular assist device inflow and outflow cannula positioning using a naturally shaped ventricle and aortic branch. *Artif. Organs* 34:798–806, 2010.

[15]Leo, H. L., L. P. Dasi, J. Carberry, H. A. Simon, and A. P. Yoganathan. Fluid dynamic assessment of three polymeric heart valves using particle image velocimetry. *Ann. Biomed. Eng*. 34:936–952, 2006.
[16]Lieber, B. B., V. Livescu, L. N. Hopkins, and A. K. Wakhloo. Particle image velocimetry assessment of stent design influence on intra-aneurysmal flow. *Ann. Biomed. Eng*. 30:768–777, 2002.
[17]Medero, R., C. Hoffman, and A. Roldán-Alzate. Comparison of 4D flow MRI and particle image velocimetry using an in vitro carotid bifurcation model. *Ann. Biomed. Eng*. 46:2112–2122, 2018.
[18]Morino, T., T. Tanoue, S. Tateshima, F. Vinuela, and K. Tanishita. Intra-aneurysmal blood flow based on patient-specific CT angiogram. *Exp. Fluids* 49:485–496, 2010.
[19]Raffel, M., C. E. Willert, S. Wereley, and J. Kompenhans. Particle Image Velocimetry. Berlin: Springer, p. 448, 2007.
[20]Ruedinger, K. L., D. R. Rutkowski, S. Schafer, A. Roldán-Alzate, E. L. Oberstar and C. Strother. Impact of image reconstruction parameters when using 3D DSA reconstructions to measure intracranial aneurysms. *J. Neurointerv. Surg*. 10:285–289, 2017.
[21]Rutkowski, D. R., R. Medero, F. J. Garcia, and A. Roldán-Alzate. MRI-based modeling of spleno-mesenteric confluence flow. *J Biomech* 88:95–103, 2019.
[22]Scholz, P., I. Reuter, and D. Heitmann. PIV measurements of the flow through an intake port using refractive index matching. In: 16th International Symposiyum on Applications of Laser Techniques to Fluid Mechanics, 2012.
[23]Smith, R. F., B. K. Rutt, and D. W. Holdsworth. Anthropomorphic carotid bifurcation phantom for MRI applications. *J. Magn. Reson. Imaging* 10:533–544, 1999.
[24]Solaris®. Technical data sheet, clear silicone encapsulating Rubber, Smooth-On. Macungie, PA.
[25]Stoiber, M., T. Schlöglhofer, P. Aigner, C. Grasl, and H. Schima. An alternative method to create highly transparent hollow models for flow visualization. *Int. J. Artif. Organs* 36:131–134, 2013.
[26]Sulaiman, A., L. Boussel, F. Taconnet, J. M. Serfaty, H. Alsaid, C. Attia, L. Huet, and P. Douek. In vitro non-rigid life-size model of aortic arch aneurysm for endovascular prosthesis assessment. *Eur. J. Cardio-Thoracic Surg*. 33:53–57, 2008.
[27]SYLGARDTM 184. Technical data sheet, The Dow Corning Company. Midland, MI.
[28]Taylor, T. W., and T. Yamaguchi. Three-dimensional simulation of blood flow in an abdominal aortic aneurysm using steady and unsteady computational methods. *J. Biomech. Eng*. 22:229–232, 1992.
[29]Töger, J., S. Bidhult, J. Revstedt, M. Carlsson, and E. Heiberg. Independent validation of four-dimensional flow MR velocities and vortex ring volume using particle imaging velocimetry and planar laser-Induced fluorescence. *Magn. Reson. Med*. 75:1064–1075, 2016.
[30]Wohl, C. J., F. L. Palmieri, J. W. Hopkins, A. M. Jackson, J. W. Connell, Y. Lin, and A. A. Cisotto. Flexible micropost arrays for shear stress measurement. In: NASA Scientific Technical Information, pp. 1–33, 2015.
[31]Wright, S. F., I. Zadrazil, and C. N. Markides. A review of solid–fluid selection options for optical-based measurements in single-phase liquid, two-phase liquid–liquid and multiphase solid–liquid flows. *Exp. Fluids* 58:1–39, 2017.
[32]Yagi, T., A. Sato, M. Shinke, S. Takahashi, Y. Tobe, H. Takao, Y. Murayama, and M. Umezu. Experimental insights into flow impingement in cerebral aneurysm by stereoscopic particle image velocimetry: Transition from a laminar regime. *J. R. Soc. Interface* 10:1–14, 2013.
[33]Yazdi, S. G., P. H. Geoghegan, P. D. Docherty, M. Jermy, and A. Khanafer. A review of arterial phantom fabrication methods for flow measurement using PIV techniques. *Ann. Biomed. Eng*. 46:1697–1721, 2018.
[34]Yip, R., R. Mongrain, A. Ranga, J. Brunette, and R. Cartier. Development of anatomically correct mock-ups of the aorta for PIV investigations. In: Proceedings of the Canadian Design Engineering Network Conference, pp. 1–10, 2004.